ELSEVIER

Journal of Contaminant Hydrology 33 (1998) 211–230

JOURNAL OF
Contaminant
Hydrology

Effect of water content on solute transport in a porous medium containing reactive micro-aggregates

Claudia Fesch [a], Peter Lehmann [b], Stefan B. Haderlein [a,*], Christoph Hinz [b,1], René P. Schwarzenbach [a], Hannes Flühler [b,2]

[a] *Institute for Aquatic Sciences and Water Pollution Control (IGW), ETHZ and Swiss Federal Institute for Environmental Sciences and Technology (EAWAG), CH-8600 Dübendorf, Switzerland*
[b] *Institute of Terrestrial Ecology (ITÖ), ETHZ, CH-8952 Schlieren, Switzerland*

Abstract

The water content of porous media may substantially affect the transport behaviour of conservative and sorbing solutes. Physical processes potentially involved include alterations of the flow velocities, flow patterns, or of accessible surface sites. We performed column experiments using a synthetic porous medium, in which a substantial part of the sorption sites was concentrated in regions within small grained aggregates that were accessible only by diffusion, a feature often found in natural soils and sediments. We investigated the transport of solutes exhibiting very different sorption characteristics under steady state conditions at different water contents of the porous medium. The tracers used were either nonreactive, partitioned into organic matter or sorbed specifically and nonlinearly to clay minerals. Hydrodynamic dispersion generally increased with decreasing water content, reflected by the breakthrough curves (BTCs) of conservative and only slightly sorbing tracers, which exhibited stronger spreading and early breakthrough of the fronts at lower water saturation. Nonlinear sorption and nonequilibrium mass transfer between the mobile region and the immobile water present within the aggregates dominated the BTCs of the strongly sorbing tracer at all degrees of water saturation, and, thus, rendered the effects of increased hydrodynamic dispersion negligible. Due to a relative increase in the ratio of sorption sites per water volume, the retardation of this tracer distinctly increased at low water contents of the porous medium. Solute transport of all tracers was successfully simulated with an advective–dispersive transport model that considered the respective sorption behaviour and retarded intra-ag-

* Corresponding author. Fax: +41-1-823-54-71; e-mail: haderlein@eawag.ch
[1] Present address: Institute of Soil Science and Forest Nutrition, University of Göttingen, Büsgenweg 2, D-37077 Göttingen, Germany.
[2] Also corresponding author. Fax: +41-1-633-11-23; e-mail: fluehler@ito.umnw.ethz.ch.

PII S0169-7722(98)00071-0

gregate diffusion as predominant processes. All parameter values of the model had been determined previously in independent experiments under completely saturated conditions. Our results demonstrate that a well parameterised transport model that was calibrated under completely saturated conditions was able to describe rate-limited advective-dispersive transport of reactive solutes also under unsaturated steady-state conditions. Enhanced relative retardation of strongly sorbing compounds under such conditions is likely to affect biological and chemical transformation processes of these compounds.

Keywords: Unsaturated zone; Diffusion; Advection; Adsorption; Kinetics; Dispersivity

1. Introduction

The transport and fate of organic chemicals in the subsurface is affected by various physical and chemical processes including advective and diffusive transport, hydrodynamic dispersion, ad- and desorption, as well as chemical and biological transformations (see reviews of Jury and Flühler, 1992; Brusseau, 1994). Limited bioavailability due to sorption to the solid matrix was shown to be one of the key factors restricting the degradation of pollutants in *saturated* porous media (Ogram et al., 1985; Miller and Alexander, 1991; McBride et al., 1992; Harms and Zehnder, 1995; Martins and Mermoud, 1998). In addition to hydrophobic partitioning into organic matter, certain organic solutes may also adsorb to mineral surfaces which often gives rise to nonlinear sorption isotherms (Zachara et al., 1990; Stone et al., 1993; Haderlein et al., 1996). Since in natural porous media reactive sorbents are typically associated with fine materials which predominate in regions where advective flow is insignificant (Greenland and Hayes, 1981), recent research has focused on rate-limited mass exchange with such immobile regions (Bouchard et al., 1988; Ball and Roberts, 1991; Young and Ball, 1994; Haggerty and Gorelick, 1995; Hu and Brusseau, 1996; Fesch et al., 1998). Even a very small fraction of such immobile regions may strongly affect the transport of *reactive* solutes if a significant fraction of the reactive sorption sites is located therein (Young and Ball, 1994; Fesch et al., 1998). In *unsaturated* systems the pattern of water flow may change significantly with the degree of saturation of the porous medium. Due to capillary forces, small pores tend to remain water-filled, whereas the larger pores may drain readily. This relative increase of the fraction of immobile water may increase dispersion (e.g., Nielsen and Biggar, 1961; Gaudet et al., 1977; De Smedt and Wierenga, 1984; Maciejewski, 1993) or lead to more variability of the unsaturated conductivity (Russo and Dagan, 1991). Moreover, an absolute increase in immobile regions may result from pores that are isolated from the main flow field (Bond and Wierenga, 1990).

While transport of nonreactive solutes has been studied extensively in saturated and unsaturated porous media, much less is known about the factors that control the transport of *sorbing* solutes in *un*saturated systems (e.g., Zurmühl et al., 1991; Chen et al., 1996). As schematically illustrated in Fig. 1, reactive surfaces such as clay minerals or iron and manganese oxides may not be evenly distributed within natural porous media and the accessibility of such sites for reactive solutes may vary with water saturation. If, e.g., the number of sorption sites per unit volume of water-filled pore space varies with the water content, the retardation of solutes that interact with these surfaces is also

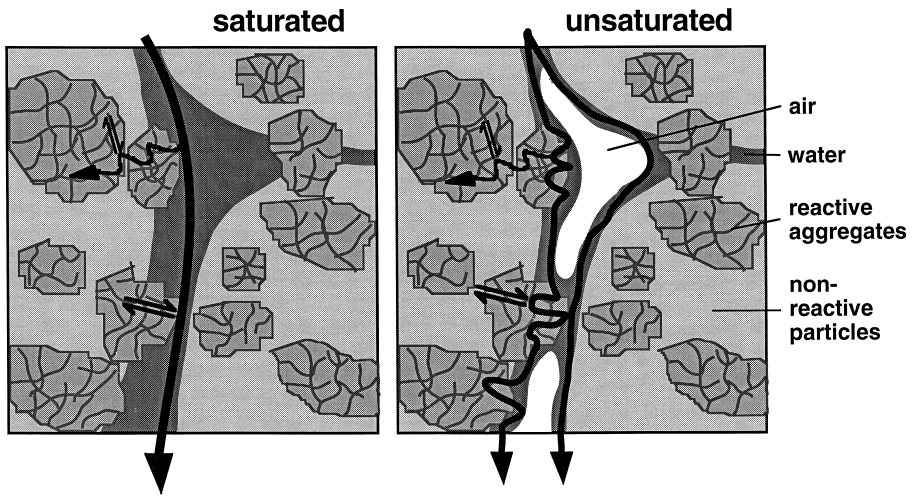

Fig. 1. Schematic illustration of a section of a porous medium that contains nonreactive coarse particles (lightest grey) and reactive fine particles that are partly aggregated thus establishing immobile regions with diffusive solute flux only (grey with dark lines). White areas represent air in the unsaturated system. Flow patterns may vary with the degree of water saturation of the porous medium. Single arrows represent advective flow (thick line) and diffusional solute flux into the immobile regions (thin lines). In both regions sorption may take place (double arrows).

expected to vary with water saturation. Thus, for the transport of reactive solutes, the relative importance of hydrodynamic and chemical processes may change with the water content of the porous medium.

In this work, we examined the effect of water content on solute transport in a porous medium consisting of a mixture of solids with different sorptive properties. In particular, transport of a reactive tracer (1,3-dinitrobenzene; DNB) that strongly and nonlinearly interacts with clay minerals (Haderlein et al., 1996) was studied in laboratory column experiments. The solid matrix consisted of quartz sand and small grained microporous aggregates of clay mineral sorbents glued together with an organic polymer. The immobile regions within these aggregates made up only a very small fraction of the total porosity of the porous medium but hosted a considerable portion of the reactive mineral surfaces present. To probe for hydrodynamic effects only, thiourea was used as a nonreactive tracer. In addition, *p*-cresol was used to probe for hydrophobic partitioning into organic matter. Steady-state miscible displacement experiments were carried out at different water contents and flow conditions. Breakthrough curves (BTCs) of the various tracers were measured and used to identify and quantify the different processes influencing solute transport. BTCs were analysed with a transport model developed and calibrated for completely *saturated* conditions in columns that contained the same type of clay aggregates. In addition to hydrodynamic processes the model is able to deal with nonlinear sorption and retarded diffusion into immobile regions. This allowed us to study the effects of water saturation on the transport of conservative as well as nonlinearly sorbing solutes, and moreover, to evaluate the applicability of the model for unsaturated porous media.

2. Materials and methods

2.1. Column experiments

Fig. 2 shows schematically the experimental set-up. All experiments were conducted at 20 ± 1.5°C. The column was made from transparent polyvinyl chloride (PVC) and had a length of 13.5 cm and a diameter of 5.3 cm. Solutions from two reservoirs were supplied at a constant flux using a pinion pump (MV-pump system, Ismatec, Switzerland). A two-way valve (Omnifit, United Kingdom) allowed switching between the reservoirs without flow interruption. A sprinkling system delivered water to the top of the column, which was open to the atmosphere, maintaining a uniform and fairly constant irrigation rate over the whole cross-section of the column (Dury et al., 1998). To establish steady-state flow conditions with a uniform water content (see below), suction was applied to the porous plate at the bottom of the column (diameter 6.2 cm; air entry value of > 100 cm) by adjusting the level of the column outlet tubing, which was

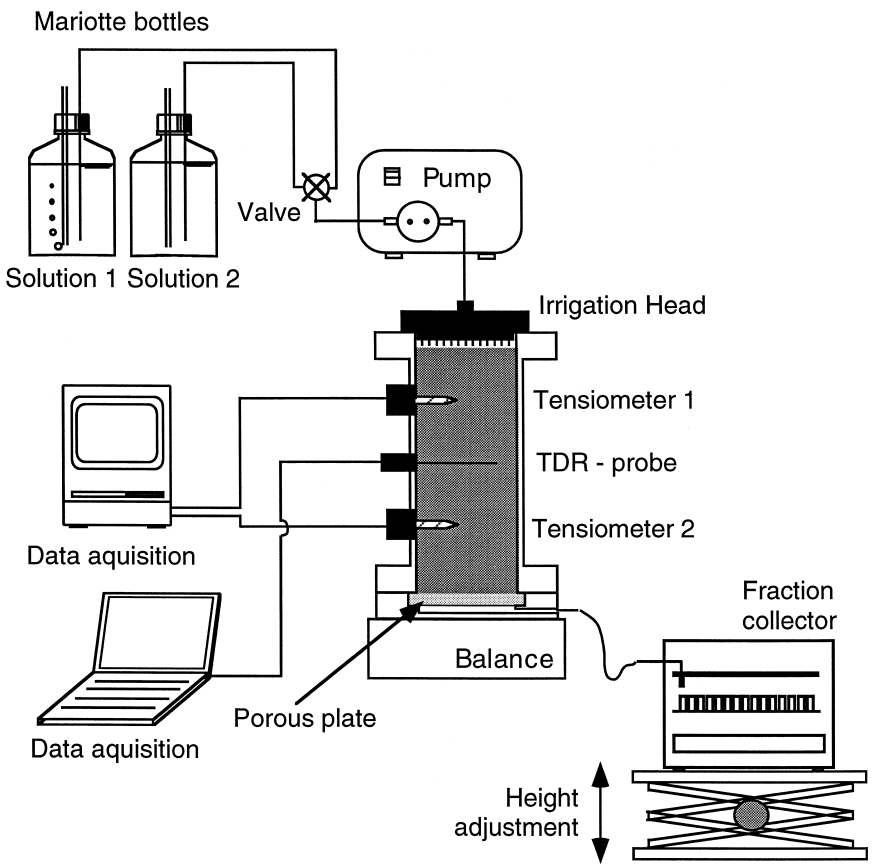

Fig. 2. Set-up of the steady-state unsaturated miscible displacement column experiments.

Table 1
Hydraulic conditions of the miscible displacement column experiments

Water content[a] Θ [$cm^3\ cm^{-3}$]	Water saturation[a] [$cm^3\ cm^{-3}$]	Pore water velocity[a] ν [$cm\ min^{-1}$]	Dispersivity[b] λ [cm]
0.319	0.86	0.09	0.1
0.353	0.96	1.10	0.1
0.242	0.66	0.96	0.15
0.205	0.56	0.54	0.35
0.168	0.45	0.18	1.3

[a]Mean values are reported with standard deviations of 3–6% due to irregular fluctuations of the water content, especially during long lasting experiments.
[b]Calculated from dispersion coefficients, D, fitted to the BTCs of the conservative tracer thiourea (Eq. (19)).

connected to a fraction collector (Gilson 203B, Gilson, USA). The flow rate and the water content were measured gravimetrically. The flow velocities ranged from 0.09 cm min^{-1} to 1.10 cm min^{-1} and the water contents from 45 to 96% saturation (Table 1).

The column was packed with the dry sorbent and was slowly saturated from bottom to top. The system was conditioned with 0.1 M KCl in order to obtain homoionic K^+-clay which enhances the sorption of the reactive nitroaromatic tracer (Haderlein and Schwarzenbach, 1993) followed by equilibration with 50 pore volumes of 0.01 M KCl. Table 1 summarises the hydraulic parameter values of the miscible displacement experiments. For each set of conditions, tracer BTCs were measured independently in single solute experiments. Due to air entrapment, maximum values for reversible water saturation of the porous medium under the flow conditions applied were 96 and 86%, respectively. Maximum saturation was higher at high water flow rates, in accordance to findings of Faybishenko (1995). Water content of the matrix was monitored with a TDR-probe (three parallel rods, 5.4 cm in length, 0.2 cm in diameter, and 0.8 cm spaced) in the centre of the column (data logger: CASMI, Poland). Matrix potential heads were measured 4 cm and 11 cm above the porous plate with two tensiometers (1.5 cm in length, 0.7 cm in diameter) equipped with pressure transducers (PR-9, Keller, Winterthur, Switzerland; data monitoring: Workbench, Strawberry tree, USA). The rates of the inflow and the outflow were equal and the matrix potential head measured within the column was equal to the suction head applied at the porous plate. The difference between the values of the matrix potential heads of the two tensiometers was less than 1 cm for all experiments indicating uniform water content. However, the sprinkling system used for solute delivery in our system generated some irregular fluctuations of the steady state flow conditions (3–6%, see Table 1).

2.2. Sorbents

The porous medium consisted of 17% fine (80–250 μm) and 83% coarse quartz sand (250–1250 μm, Zimmerli Mineralwerk, Zürich, Switzerland) with the fine sand being coated with aggregates of montmorillonite ($\approx$ 1–20 μm, for details see Fesch et al., 1998). This distribution of grain size allowed to cover a wide range of unsaturated flow

Table 2
Names, abbreviations and some pertinent properties of the tracer solutes (octanol/water partitioning coefficient, K_{ow}, acidity constant, K_a, wavelength of maximum UV-light absorption, λ_{max}, and extinction coefficient, ε_{max}, at λ_{max})

Compound	Abbreviation	log K_{ow}	pK_a	λ_{max} [nm]	ε_{max} [M^{-1} cm^{-1}]
thiourea	thiourea	≈ -1[a]	1.18[c]	235	11 000
4-methylphenol	*p*-cresol	1.92[a]	10.26[d]	278	1700
1,3-dinitrobenzene	1,3-DNB	1.49[b]	–	242	15 600

[a] Hansch and Leo (1979).
[b] Values calculated by means of π-fragment constants (Fujita, 1983) and structure factors (Leo et al., 1971).
[c] pK_a of the protonated species ($I = 0.1$ M), Martell and Smith (1982).
[d] $I = 0.05$ M, Serjeant and Dempsey (1979).

conditions (see Table 1). The specific surface area of the resulting matrix was 1.6 m^2 g^{-1} as determined by BET N_2 adsorption (Milestone 100, Carlo Erba Strumentazione) and the total fraction of clay was 0.66% (w/w). The organic carbon content (f_{oc}), which was measured with a CHN analyser (Heraeus CHN-Rapid, Heraeus Instrument, Switzerland), was 0.03%.

2.3. Solutes

Table 2 summarises the names, abbreviations and some important properties of the tracers. All compounds were purchased from Fluka (Buchs, Switzerland) in the highest purity available ($\geq 97\%$) and were used as received. As a nonreactive tracer thiourea was used (Unger, 1989). 1,3-Dinitrobenzene (DNB) was chosen as a reactive tracer because it sorbs strongly and nonlinearly to clay minerals exhibiting a saturation type sorption isotherm (Haderlein et al., 1996). *p*-Cresol was used as a hydrophobic partitioning tracer that exclusively sorbed to the organic polymer glue (polyvinylalcohol, PVA) present in the matrix. Since *p*-cresol and DNB are of similar hydrophobicity, the contribution of hydrophobic partitioning to the overall sorption of DNB in the model system could be estimated from the sorption of *p*-cresol. Besides sorption characteristics, the selection criteria for the tracers included ease of measurement (i.e., significant UV absorption) and absence of charge (to exclude such interactions as cation exchange or electrostatic repulsion). Aqueous-phase concentrations of the tracers were measured photometrically (PU 8620, Philips Technology, GB) at the respective wavelengths of maximum absorption (see Table 2).

2.4. Data analysis and modeling

Since the experiments were carried out under steady-state flow conditions of fairly uniform water content throughout the column (see Section 2.1), transport models developed for saturated conditions could be used to describe the BTCs by correcting for the water content and the flow velocity. BTCs of the conservative and hydrophobic tracers were analysed with the computer code CXTFIT (Parker and van Genuchten,

1984; Toride et al., 1995). Dispersion coefficients and retardation factors of conservative and hydrophobic tracers were estimated using both the one-region and the two-region models available in CXTFIT. Both approaches resulted in very similar parameter values since the fraction of immobile water was negligible for the conservative and the only slightly sorbing tracer. The nonlinear least-squares inversion method implemented in CXTFIT involves an analytical solution of the one-dimensional advection dispersion equation (ADE). Since analytical solutions are not available for the transport of nonlinearly sorbing solutes, the BTCs of DNB were analysed numerically with the computer code AQUASIM (Reichert, 1994a; Simon and Reichert, 1997). The configuration used was a two-region model considering advection, hydrodynamic dispersion, (retarded) diffusion into and within immobile regions as well as nonlinear sorption in both the advective and the immobile regions. The model was implemented numerically by discretizing the immobile region into n different zones. AQUASIM allows to calculate simultaneously multiple BTCs without noticeable effects of numerical diffusion (Reichert, 1994b), which was confirmed by the similarity of parameter values for BTCs of the conservative tracer obtained with CXTFIT and AQUASIM, respectively (data not shown). A major assumption of our approach in unsaturated column experiments was that the water content varied only in the mobile region of the porous medium while the immobile region within the aggregates was assumed to be water-filled at all our experimental conditions (see Fig. 1). This is in agreement with findings of Grathwohl and Reinhard (1993) who found intra-particle diffusion rates in moist but unsaturated porous media to be independent of the water content. A detailed description of this model and its application to solute transport under completely saturated condition is given in Fesch et al. (1998). Its major features can be summarised as follows (for definition of parameters see the appendix):

The total porosity of the column, ϕ, is divided into the porosity of the mobile region, ϕ_{mob}, and that of the immobile region, ϕ_{im}:

$$\phi = \phi_{mob} + \phi_{im} \tag{1}$$

where:

$$\phi_{im} = f_{im} \cdot \phi \tag{2}$$

Accordingly, the total water content, θ, is given as:

$$\theta = \theta_{mob} + \theta_{im} \tag{3}$$

Assuming all pores of the immobile regions to be water-filled at all water contents considered (see above), the water content of the immobile region is equal to the corresponding porosity and thus,

$$\theta_{mob} = \theta - \phi_{im} \tag{4}$$

Since sorption takes place in both regions, the total solute concentrations expressed as total mass of solute per liquid volume are given by:

$$C_{mob}^{tot} = C_{mob} + \frac{\rho_b}{\theta_{mob}} S_{mob} \tag{5}$$

$$C_{im}^{tot} = C_{im} + \frac{\rho_b}{\theta_{im}} S_{im} \tag{6}$$

Due to diffusive processes, the solute penetrates into the fine pores of the immobile region. The solute flux, F_{im}, along the spatial coordinate, z, of these fine pores is described by Fick's first law of diffusion:

$$F_{im}(z) = -a(z) D_0 \frac{\partial C_{im}}{\partial z}(z) \tag{7}$$

where *a(z)* is the sum of the cross-sectional areas of all pores of the immobile region per unit column volume. It is measured perpendicular to the direction of diffusion into the pores, and may vary with the spatial coordinate, z, along the pores. The porosity of the immobile region is given by:

$$\phi_{im} = \int_0^d a(z)\, dz \tag{8}$$

where d is the maximum length of the pores of the immobile region. Note that the parameters f_{im} and d are correlated. Based on the size of the clay aggregates used (Fesch et al., 1998), a fixed value of $d = 100\ \mu$m was chosen to estimate a unique value of f_{im}. The total sorbed-phase solute concentration in the immobile region is given as:

$$S_{im} = \int_0^d s_{im}(z)\, dz \tag{9}$$

where $s_{im}(z)$ is the sorbed-phase solute concentration per unit pore depth, z, of the immobile region, leading to the total immobile solute concentration, C_{im}^{tot}, at the depth z:

$$C_{im}^{tot}(z) = C_{im}(z) + \frac{\rho_b}{a(z)} s_{im}(z) \tag{10}$$

The transport equations in the mobile and immobile regions, respectively, are given as:

$$\frac{\partial C_{mob}^{tot}}{\partial t} = -\nu \frac{\partial C_{mob}}{\partial x} + D \frac{\partial^2 C_{mob}}{\partial x^2} - \frac{F_{im}(0)}{\theta_{mob}} \tag{11}$$

$$\frac{\partial C_{im}^{tot}}{\partial t} = \frac{1}{a(z) A} \frac{\partial}{\partial z} \left(a(z) A D_0 \frac{\partial C_{im}}{\partial z} \right) \tag{12}$$

with the boundary conditions

$$C_{im}(0) = C_{mob} \tag{13}$$

$$\frac{\partial C_{im}}{\partial z}(d) = 0 \tag{14}$$

Based on results of batch sorption experiments, nonlinear sorption of the solute in both regions was described by a Langmuir–Freundlich type isotherm:

$$S_{mob}(C_{mob}) = S_{max,mob} \frac{K_{LF} C_{mob}^{\alpha}}{1 + K_{LF} C_{mob}^{\alpha}} \tag{15}$$

$$S_{im}(C_{im}) = S_{max,im} \frac{K_{LF} C_{im}^{\alpha}}{1 + K_{LF} C_{im}^{\alpha}} \tag{16}$$

The isotherm parameters, α and K_{LF}, were determined in batch experiments and were set equal for both regions. The maximum sorbed-phase solute concentrations, $S_{max,mob}$ and $S_{max,im}$, represent the total amount of sorption sites available in the mobile and the immobile region, respectively. It was shown earlier (Fesch et al., 1998) that the immobile regions in our systems were located within the micro-pores of the clay aggregates (Fig. 1), amounting to only $< 0.2\%$ of the column porosity. However, a considerable fraction of the clay sorption sites (10–30%) are located within this small volume fraction. The distribution of the sorption sites within the immobile region as well as the geometry are unknown. However, different empirical functional dependencies of *a(z)* and $s_{im}(z)$ were tested to obtain an approximation of the geometry and the site distribution within the immobile region of a certain porous medium (Fesch et al., 1998). The cross-sectional pore area of these immobile regions, *a(z)*, was found to decrease with pore depth whereas the sorption site density, $s_{max,im}(z)$, increased. Best descriptions were obtained with the following empirical functions (Fesch et al., 1998):

$$a(z) = \text{const} \cdot e^{-\gamma z} \tag{17}$$

$$s_{max,im}(z) = \text{const} \cdot (\kappa z^2 + 1) \tag{18}$$

where γ and κ are auxiliary parameters that were fitted (Table 3), while the values of the constant, const, result from Eqs. (8) and (9). The *simultaneous* fitting of multiple BTCs that covered a wide range of time scales allowed to describe the whole set of experiments with a *single* set of at most five fitted parameters ($S_{max,mob}$, $S_{max,im}$, f_{im}, γ, κ) (see Fesch et al., 1998, for more details).

Table 3
Comparison of parameter values used to describe the BTCs of the reactive tracer DNB in the column systems of this and the previous study[a]

Parameter	Determined by	Previous study[a]	This study
α	in situ adsorption isotherm	0.57	item
K_{LF}	in situ adsorption isotherm	0.12 l^{α} $\mu mol^{-\alpha}$	item
$S_{max,mob}$	fitted on basis of the in situ adsorption isotherm	264 μmol kg^{-1}	45 μmol kg^{-1}[b]
$S_{max,im}$	fitted on basis of the in situ adsorption isotherm	250 μmol kg^{-1}	item
$S_{max,im}$ (2)	fitted via Eq. (18)	$\kappa = 1122$ cm^{-2}	item
a (z)	fitted via Eq. (17)	$\gamma = 727$	item
f_{im}	fitted, yielding from *d*	$1.6 \cdot 10^{-3}$ cm cm^{-3}	$2.7 \cdot 10^{-4}$ cm cm^{-3}[b]
d	REM images of aggregate size	100 μm	item
D_0 (22°C)	estimated on the basis of the molar volume of the solutes[c]	$4.8 \cdot 10^{-4}$ cm^2 min^{-1}	item

Parameter values for nonlinear sorption (Langmuir–Freundlich type), distribution of the sorption sites and geometry of the immobile regions were equal in both systems. $S_{max,mob}$ and f_{im} were adjusted according to the lower fraction of clay aggregates in the columns used here (Table 4).

[a] Fesch et al. (1998).

[b] Adjusted to the lower fraction of aggregated clay particles used in this study.

[c] Schwarzenbach et al. (1993).

Table 4
Comparison of physical properties and parameter values of the column systems (see text, Section 2.4)

Parameter	Abbreviation [units]	Previous study[a]	This study
length	ℓ [cm]	12.2	13.5
diameter	[cm]	1.0	5.3
cross sectional area	A [cm^2]	0.8	22.0
bulk density	ρ_b [g cm^{-3}]	1.4	1.7
porosity	ϕ [cm^3 cm^{-3}]	0.47	0.37
fraction montmorillonite	[% by weight]	3.8	0.66
grain sizes	[μm]	80–200	80–1250
velocities	ν [cm min^{-1}]	0.03–3.0	0.09–1.0
water saturation	[% by volume]	100	45–96

[a] Fesch et al. (1998).

Compared to the experiments conducted under completely saturated conditions (Fesch et al., 1998), in this study a bigger column system had to be used (Section 2.1 and Table 4) in order to establish unsaturated flow conditions and to monitor water content and matrix potential heads within the column. It should be pointed out, however, that, because the column contained the very same clay aggregates, the sorption and diffusion processes were described using the same sorption related parameter values as obtained in the smaller column of the previous work. Thus, all model calculations presented here were true predictions, i.e., they were simulation runs without any parameter fitting. Table 4 compares the properties of the two different column systems, and Table 3 shows the parameter values that were used to describe the sorption, the geometry of the immobile region, and the sorption site distribution therein.

3. Results and discussion

3.1. Conservative tracer

BTCs of thiourea are used to discuss the hydrodynamic flow regime for the various experimental conditions (Fig. 3). The effect of flow velocity on the BTCs was studied at quasi-saturated conditions of 96 and 86% water saturation. The solute BTCs were almost identical when plotted as a function of effective pore volumes of solution percolated through the porous medium (Fig. 3a). Very similar BTCs were obtained for both high and low pore water velocities. This indicates that nonequilibrium processes were negligible for the transport of thiourea within the time frame of these experiments. However, the fronts of the BTCs were slightly asymmetric, likely due to a somewhat irregular flow pattern within the porous plate at the bottom of the column. Control experiments of solute BTCs through the porous plate alone without column packing confirmed this interpretation (data not shown). However, this non-ideal flow pattern through the porous plate had only a very minor impact on the calculated dispersion coefficients of the various tracers studied, and, thus, will be neglected in the following discussion.

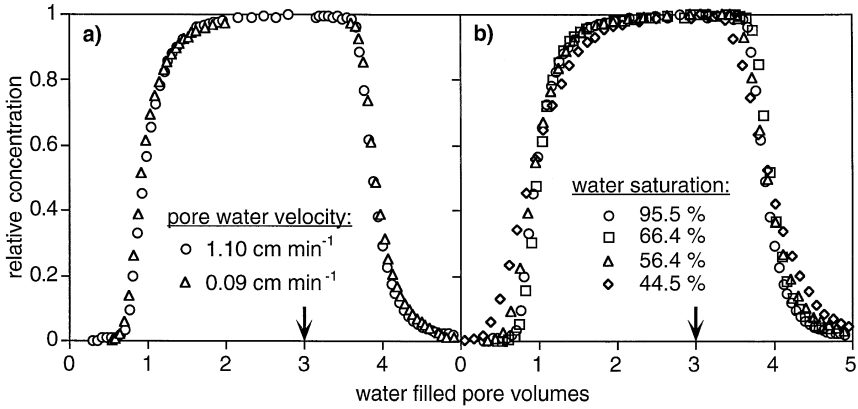

Fig. 3. Measured BTCs of the conservative tracer thiourea. Arrows indicate duration of input pulse ($C_0 = 60$ μmol l^{-1}; see Table 1 for hydraulic conditions). (a) Similar BTCs at different pore water velocities under quasi-saturated conditions indicate quasi-equilibrium conditions. (b) With decreasing water content fronts of BTCs are less sharp and exhibit early breakthrough.

Fig. 3b shows BTCs of thiourea as a function of water content. With decreasing water content of the porous medium, the BTCs spread out and solute breakthrough occurred earlier. The dispersivity, λ, of each solute pulse was calculated from the fitted hydrodynamic dispersion coefficient, D, assuming a linear relationship between D and the pore water velocity, ν, (Bear, 1972; Jury et al., 1991):

$$\lambda = \frac{D}{\nu} \tag{19}$$

The dispersivities increased with decreasing water content (Table 1) indicating that the air filled pore space increased the tortuosity of the solute flow path, which corresponds to the experimental findings of Maciejewski (1993) and the network simulations of Sahimi et al. (1986). Thus, for conservative solutes such as thiourea, the degree of water saturation had a distinct impact on the transport behaviour in our system.

3.2. Effect of hydrophobic partitioning

To probe for the effect of water saturation on the extent of hydrophobic partitioning of solutes to the organic matter present in the porous medium, we measured BTCs of *p*-cresol (Fig. 4). Generally, the retardation of *p*-cresol was low ($R < 1.1$), consistent with the low content of organic carbon ($f_{oc} = 0.03\%$) of the matrix. This result also validates our experimental set-up and procedures since it shows the absence of significant hydrophobic partitioning to the hardware of the system. At all flow velocities and degrees of saturation studied, hydrophobic partitioning had only a minor impact on solute transport. Similar to the results obtained with thiourea, the BTCs of *p*-cresol were equivalent at low and high pore water velocities under quasi-saturated conditions (Fig. 4a). This indicates that the transport of *p*-cresol was not significantly influenced by

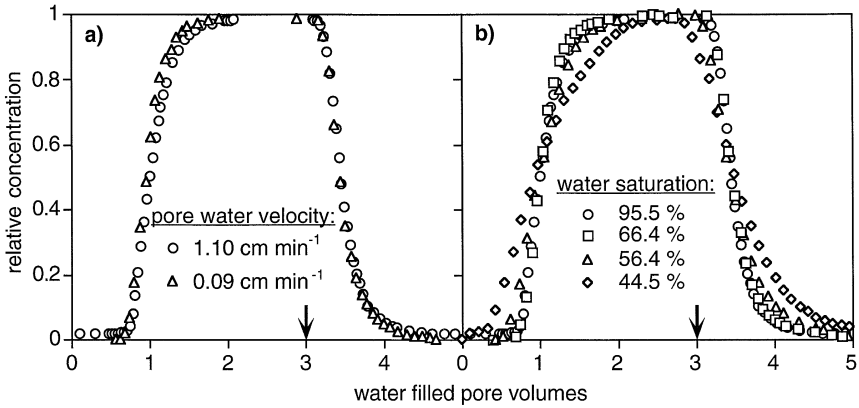

Fig. 4. Measured BTCs of the hydrophobic tracer *p*-cresol. Arrows indicate duration of input pulse ($C_0 = 250$ μmol l^{-1}; see Table 1 for hydraulic conditions). (a) Similar BTCs at different pore water velocities under quasi-saturated conditions indicate quasi-equilibrium conditions. (b) With decreasing water content fronts are less sharp and exhibit early breakthrough.

nonequilibrium processes. The dispersivity also increased with decreasing degree of water saturation, which was reflected by increased spreading of the fronts (Fig. 4b). Since the partitioning tracer showed an almost conservative behaviour, retardation due to hydrophobic partitioning into organic matter was assumed to be insignificant for DNB, which has a similar hydrophobicity as *p*-cresol but sorbs strongly to clay minerals.

3.3. Reactive tracer

In contrast to thiourea and *p*-cresol, the BTCs of DNB were strongly retarded and had sharp adsorption but strongly tailing desorption fronts (Fig. 5). These features are characteristic for solutes exhibiting convexly shaped sorption isotherms (Bürgisser et al., 1993; Helfferich and Carr, 1993) such as DNB, which sorbs strongly to clay minerals (Haderlein et al., 1996). At nearly saturated conditions a decrease in pore water velocity resulted in stronger retardation and stronger spreading of the DNB BTCs (Fig. 6a). These effects are in accordance with nonequilibrium mass transfer due to retarded DNB diffusion within the clay aggregates. Note that the presence of nonequilibrium processes has been shown in interrupted flow experiments (Fesch et al., 1998), and that chemical nonequilibrium processes due to rate limiting ad- or desorption of DNB at clay surfaces can be ruled out (Haderlein et al., 1996; Weissmahr et al., 1997).

Fig. 6b compares BTCs of DNB measured at different water contents of the porous medium. With decreasing water saturation, the BTCs also were retarded more strongly and the fronts were more spread. According to Eq. (20) the retardation of DNB is indeed expected to increase with decreasing water content, provided that (most of) the sorption sites remain accessible from the water filled pore space of the porous medium.

$$R = 1 + \frac{\rho_b}{\theta}\frac{\partial S(C)}{\partial C} \tag{20}$$

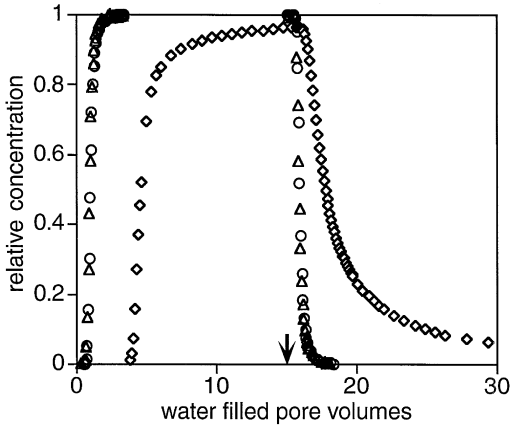

Fig. 5. Comparison of the BTCs of all tracers at 96% water saturation and a pore water velocity of 1.10 cm min^{-1} (○: thiourea; △: *p*-cresol; ◇: DNB). The arrow indicates duration of input pulse. The partitioning tracer *p*-cresol ($C_0 = 250$ μmol l^{-1}) is only slightly retarded indicating negligible hydrophobic partitioning. The BTCs of the nonlinearly sorbing DNB ($C_0 = 50$ μmol l^{-1}) show strong retardation with sharp adsorption and tailing desorption fronts. These features of the BTCs were similar at all saturation levels studied (data not shown).

These results can be rationalised when considering that the concentration of reactive surface sites increases as the water content of the porous medium declines, resulting in stronger retardation. Note that varying the water saturation of the columns not only affected the ratio of sorption sites per water volume but also the pore water velocity (see Table 1).

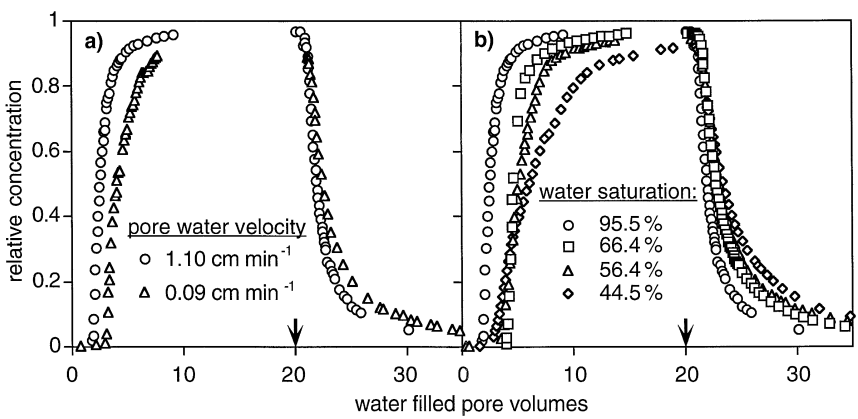

Fig. 6. BTCs of the nonlinearly sorbing tracer DNB. Arrows indicate duration of input pulse ($C_0 = 50$ μmol l^{-1}; see Table 1 for hydraulic conditions). (a) The retardation of the BTCs under quasi-saturated conditions increased with decreasing pore water velocity indicating nonequilibrium mass transfer. (b) Retardation also increased at lower water contents due to a relative increase of the ratio of reactive surface sites to water volume.

For a quantitative evaluation of the data we analysed the BTCs using the transport model outlined in Section 2.4. The BTCs of DNB were *simulated* using parameter values obtained previously from independent experiments under *completely saturated* conditions (see Tables 3 and 4). This allowed us to examine whether under *unsaturated* conditions nonlinear sorption (Langmuir–Freundlich type) and retarded diffusion within clay aggregates were also the predominant processes influencing the transport of strongly sorbing solutes such as DNB. Moreover, we could test the transferability of the calibrated model to *un*saturated conditions as well as to a different experimental set-up. We used identical parameter values describing the geometry, the distribution of the sorption sites, and the sorption isotherm within the immobile regions of the aggregates since very similar clay aggregates were present in both studies. To account for the smaller fraction of clay aggregates present in this unsaturated system, the fraction of the immobile region, f_{im}, was decreased accordingly as was the parameter value for the maximum sorbed-phase solute concentration in the mobile region, $S_{max,mob}$. The different degrees of water saturation of individual experiments were taken into account by setting the parameter value of the volumetric water content of the mobile region accordingly. The immobile regions were assumed to be completely water saturated at all water contents considered (see Section 2.4).

In a first modeling approach, the BTCs were simulated neglecting dispersive effects. Fig. 7 shows that these simulated dispersion free BTCs matched the principal features of the measured data quite well, i.e., sharp initial adsorption but tailing desorption fronts due to convexly shaped sorption isotherms and some tailing in the upper part of the adsorption front due to rate-limiting diffusive solute exchange with immobile regions. The retardation of simulated and measured BTCs increased with both decreasing pore water velocity and decreasing water content. Note that the strong retardation at low water content cannot be explained alone by lower flow rates present at these conditions. At 45% water saturation DNB was more strongly retarded than at 86% (compare Fig. 6a and b), although the pore water velocity was two times higher at 45% water saturation (see Table 1). Furthermore, from Fig. 7 it is evident that the model simulations reflected the observed spread in the otherwise sharp adsorption fronts as well as the distinctly stronger tailing of the desorption fronts with decreasing water contents, although the simulated retardation of the BTCs was slightly off the measured data and the predicted maximum solute concentrations at the column outlet were somewhat lower than the measured values. However, when comparing the model predictions with the measured BTCs, one has to keep in mind that, in contrast to the completely saturated conditions of Fesch et al. (1998), the flow rate and the water saturation varied irregularly by 3 to 6% during the unsaturated and quasi-saturated experiments.

Simulated BTCs with and without hydrodynamic dispersion terms were essentially indistinguishable (see solid and dashed lines in Fig. 7) if hydrodynamic dispersion coefficients of the conservative tracer were used. For strongly sorbing solutes the effective dispersion can get enhanced due to pore scale variation in retardation factor (Sugita and Gillham, 1995). Therefore, model simulations were performed to check whether the increased spreading of the fronts at lower water contents may be attributed to an enhanced effective dispersion. Simulated BTCs using increased dispersion coefficients showed more spread adsorption and stronger tailed desorption fronts (dashed lines

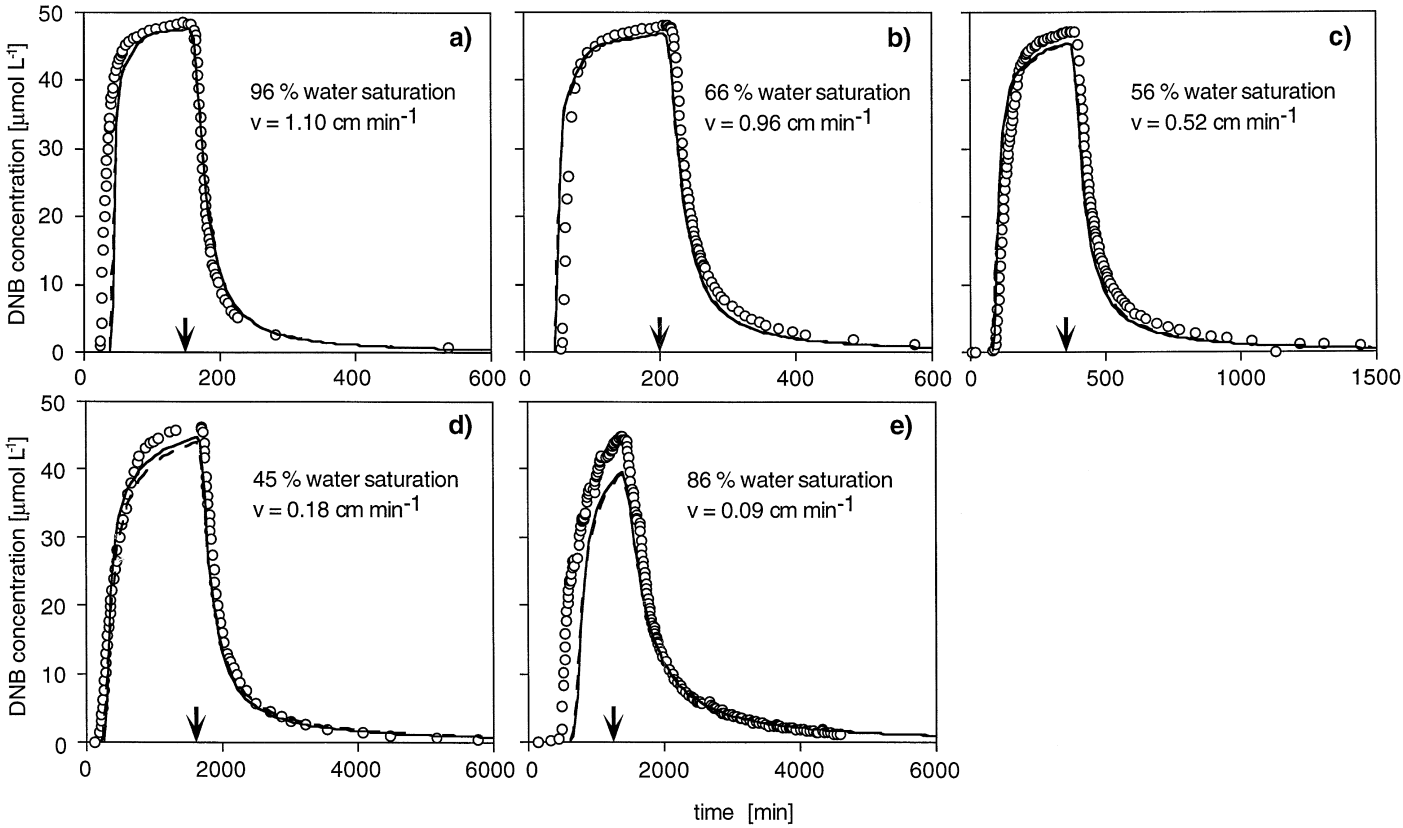

Fig. 7. BTCs of the nonlinearly sorbing tracer DNB at different water saturation levels. Arrows indicate duration of input pulses. Measured data (markers) are compared to model simulations considering (dashed lines) and neglecting (solid lines) hydrodynamic dispersion, respectively. The model included nonlinear sorption of DNB to clays according to the Langmuir–Freundlich isotherm and retarded intra-particle diffusion in the clay aggregates of the solid matrix. *All* BTCs were simulated with one single set of parameter values (Table 4), which were determined independently. Note the different scales of the abscissa in panels a–c and d–e.

in Fig. 8a). However, the retardation of the BTC fronts did not change, and the maximum output concentrations further decreased as a result of the increased dispersion. After all, in our systems, dispersion effects were minor compared to the effects of nonlinear sorption and retarded intra-aggregate diffusion.

Simulations assuming a linear sorption isotherm or those neglecting the retarded intra-aggregate diffusion of DNB largely failed to describe the data (Fig. 8b). These compilations of simulated and measured BTCs indicate that under unsaturated steady-state conditions nonlinear sorption and retarded intra-particle diffusion were also the predominant processes that controlled the transport behaviour of strongly and nonlinearly sorbing solutes in our system. The fact that the data of this study could be predicted with a transport model that was calibrated in a completely different column system suggests that the parameterisation of the model was adequate to describe physico–chemical processes within the column system as well as the distribution of reactive surface sites within the solid matrix.

Our results also suggest that some additional factors of second-order importance might have to be considered to fully understand the system. For example, the accessibility of the clay aggregates might have been affected by the presence of larger amounts of coarse sand in our system as compared to the completely saturated experiments. This may add some uncertainty to the parameter value of the fraction of immobile regions within the column packing used here. In addition, the upscaling from the small completely saturated column system (volume of 10 ml) to the larger unsaturated system (volume of 297 ml; Table 4) may involve some effects not considered in the parameter values used here.

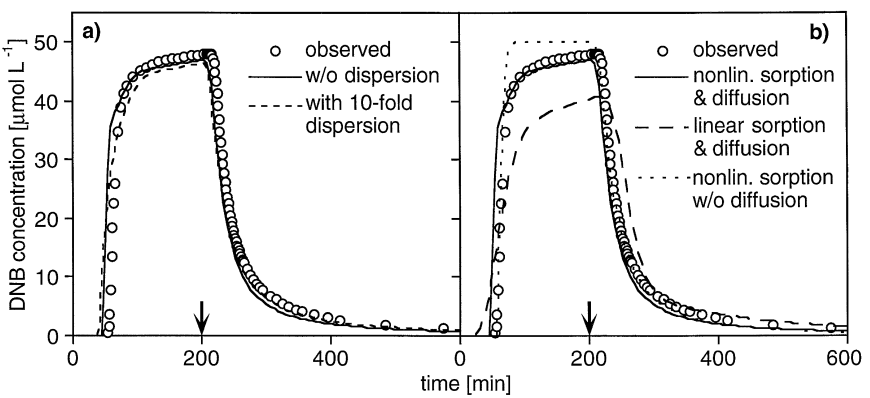

Fig. 8. Comparison of simulations of DNB BTCs to assess the relative importance of different processes ($C_0 = 50$ μmol l^{-1}; water saturation 66%; $v = 0.96$ cm min^{-1}). Arrows indicate duration of the input pulse. (a) A dispersion 10-fold higher than the measured hydrodynamic dispersion resulted in more spread adsorption and stronger tailed desorption fronts. However, the retardation of the fronts was not changed and the maximum solute concentrations were even more underestimated. (b) Simulations assuming a linear sorption isotherm or excluding diffusion into the immobile regions largely failed to describe the experimental data (dispersion neglected in these calculations).

4. Summary and conclusions

In this work, we have examined the effect of water content of a porous medium on the transport of various solutes under steady state flow conditions. The tracers used were either nonreactive, partitioned exclusively into organic matter, or sorbed strongly and nonlinearly to reactive surface sites. Miscible displacement experiments were carried out at various water contents and flow rates in a laboratory model system. Hydrodynamic dispersion generally increased with decreasing water content, reflected by the BTCs of conservative and only slightly sorbing tracers, which exhibited stronger spreading and early breakthrough of the fronts at lower water saturation. Nonlinear sorption and nonequilibrium mass transfer between the mobile region and the immobile water present within the aggregates dominated the BTCs of the strongly sorbing tracer at all degrees of water saturation, which rendered the effects of increased hydrodynamic dispersion negligible. Due to an increase in the ratio of sorption sites per water volume, the retardation of this tracer increased significantly at low water contents of the porous medium. Solute transport of all tracers was successfully simulated with a model that considered the respective sorption behaviour, advective–dispersive transport, and retarded intra-aggregate diffusion as predominant processes.

Our results demonstrate that a well parameterised transport model that was calibrated under completely saturated conditions was able to describe rate-limited advective–dispersive transport of reactive solutes under *un*saturated steady-state conditions. Our study was performed using an artificial aggregated porous medium where a fraction of the sorption sites was not instantly accessible to the solutes due to the presence of immobile regions. Such a distribution pattern of sorption sites between mobile and immobile regions is typical for many natural subsurface materials (e.g., Holmén and Gschwend, 1997). Our investigation presents experimental and theoretical evidence that in an advective–dispersive flow field retardation of strongly sorbing solutes may be substantially enhanced under unsaturated conditions due to a relative increase of the number of sorption sites per water volume. Thus, under such conditions the fraction of strongly sorbing solutes present in aqueous solution is substantially lower compared to saturated conditions, which is expected to reduce the bioavailability of the solutes (e.g., Harms and Zehnder, 1995). Conversely, surface catalysed transformation reactions such as hydrolysis (e.g., Torrents and Stone, 1991) or redox reactions (e.g., Klausen et al., 1995; Klausen et al., 1997) might be enhanced compared to reactions of solutes that are transported under saturated conditions.

5. Notation

A	cross-sectional area of column [cm^2]
$a(z)$	cross-sectional area of pores building the immobile region per unit column volume [cm^{-1}]
C_{mob}, C_{im}	solution-phase solute concentration in mobile, immobile region [$\mu mol\ l^{-1}$]
C_{mob}^{tot}, C_{im}^{tot}	total solute concentration in mobile, immobile region [$\mu mol\ l^{-1}$]

D	hydrodynamic dispersion coefficient [$cm^2\ min^{-1}$]
D_o	molecular diffusion coefficient in water [$cm^2\ min^{-1}$]
d	maximum length of the pores of the immobile regions [cm]
F_{im}	solute flux in immobile region of aggregates [$mol\ cm^{-3}\ min^{-1}$]
f_{im}	fraction of the immobile region [$l\ l^{-1}$]
f_{oc}	fraction of organic carbon [%]; [$kg\ kg^{-1} * 100$]
K_{LF}	Langmuir–Freundlich partition coefficient (an affinity (adsorption energy) parameter) [$l^{\alpha}\ \mu mol^{-\alpha}$]
ℓ	column length in x-direction [cm]
S_{mob}, S_{im}	sorbed-phase solute concentration in mobile, immobile region [$\mu mol\ kg^{-1}$]
$s_{im}(z)$	sorbed-phase solute concentration per unit pore depth z of the immobile region [$\mu mol\ kg^{-1}\ cm^{-1}$]
$S_{max,mob}$, $S_{max,im}$	maximum sorbed-phase solute concentration in mobile, immobile region [$\mu mol\ kg^{-1}$]
$s_{max,im}(z)$	maximum sorbed-phase solute concentration per unit pore depth z of the immobile region [$\mu mol\ kg^{-1}\ cm^{-1}$]
t	time [min]
ν	pore water velocity [$cm\ min^{-1}$]
x	spatial coordinate along the column [cm]
z	spatial coordinate along the pores building the immobile region [cm]
α	Langmuir–Freundlich isotherm exponent (power function) [−] $0 < \alpha \leq 1$
γ	fitting parameter [−]
ϕ	total porosity of the packed column [$l\ l^{-1}$]
ϕ_{mob}, ϕ_{im}	porosity of mobile, immobile region [$l\ l^{-1}$]
κ	fitting parameter [cm^{-2}]
λ	dispersivity [cm]
θ	total volumetric water content of the packed column [$l\ l^{-1}$]
θ_{mob}, θ_{im}	volumetric water content of mobile, immobile region [$l\ l^{-1}$]
ρ_b	bulk density of the solid matrix [$kg\ l^{-1}$]; $\rho_b = \rho_s(1-\phi)$
ρ_s	density of the solid matrix [$kg\ l^{-1}$]

Acknowledgements

We thank Olivier Dury for valuable advice and assistance during the column experiments. Organic carbon content, f_{oc}, was measured by Antonin Mares, BET measurements were carried out by Daniel Kobler. Valuable comments of the reviewers are acknowledged. The study was financed by the Board of the Swiss Federal Institutes of Technology (OPUS-project).

References

Ball, W.P., Roberts, P.V., 1991. Long term sorption of halogenated organic chemicals by aquifer materials: 2. Intraparticle diffusion. Environ. Sci. Technol. 25, 1237–1249.

Bear, J., 1972. Dynamics of Fluids in Porous Media. Elsevier, New York.
Bond, W.J., Wierenga, P.J., 1990. Immobile water during solute transport in unsaturated sand columns. Water Resour. Res. 26 (10), 2475–2481.
Bouchard, D.C., Wood, A.L., Campbell, M.L., Nkedi-Kizza, P., Rao, P.S.C., 1988. Sorption nonequilibrium during solute transport. J. Cont. Hydrol. 2, 209–223.
Brusseau, M.L., 1994. Transport of reactive contaminants in heterogeneous porous media. Rev. Geophys. 32 (3), 285–313.
Bürgisser, C.S., Cernik, M., Borkovec, M., Sticher, H., 1993. Determination of nonlinear adsorption isotherms from column experiments: An alternative to batch studies. Environ. Sci. Technol. 27, 943–948.
Chen, J.S., Mansell, R.S., Nkedi-Kizza, P., Burgoa, B.A., 1996. Phosphorus transport during transient, unsaturated water flow in an acid sandy soil. Soil Sci. Soc. Am. J. 60 (1), 42–48.
De Smedt, F., Wierenga, P.J., 1984. Solute transfer through columns of glass beads. Water Resour. Res. 20 (2), 225–232.
Dury, O., Fischer, U., Schulin, R., 1998. Dependence of the hydraulic and pneumatic characteristics of soils on a dissolved organic compound. J. Cont. Hydrol.
Faybishenko, B.A., 1995. Hydraulic behavior of quasi-saturated soils in the presence of entrapped air: laboratory experiments. Water Resour. Res. 31 (10), 2421–2435.
Fesch, C., Simon, W., Haderlein, S.B., Reichert, P., Schwarzenbach, R.P., 1998. Nonlinear sorption and nonequilibrium solute transport in aggregated porous media: experiments, process identification and modeling. J. Cont. Hydrol. 31 (3–4), 373–407.
Fujita, T., 1983. Substituent effects in the partition coefficients of disubstituted benzenes: bi-directional Hammett-type relationships. In: Taft, R.W. (Ed.), Progress in Physical Organic Chemistry. Vol. 14, Wiley, New York, pp. 75–113.
Gaudet, J.P., Jegat, H., Vachaud, G., Wierenga, P.J., 1977. Solute transfer, with exchange between mobile and stagnant water, through unsaturated soil. Soil Sci. Soc. Am. J. 41 (4), 665–671.
Grathwohl, P., Reinhard, M., 1993. Desorption of trichloroethylene in aquifer material: rate limitation at the grain scale. Environ. Sci. Technol. 27, 2360–2366.
Greenland, D.J., Hayes, M.H.B., 1981. Soil processes. In: Greenland, D.J., Hayes, M.H.B. (Eds.), The Chemistry of Soil Processes. Wiley, Chichester, pp. 1–31.
Haderlein, S.B., Schwarzenbach, R.P., 1993. Adsorption of substituted nitrobenzenes and nitrophenols to mineral surfaces. Environ. Sci. Technol. 27, 316–326.
Haderlein, S.B., Weissmahr, K.W., Schwarzenbach, R.P., 1996. Specific adsorption of nitroaromatic explosives and pesticides to clay minerals. Environ. Sci. Technol. 30 (2), 612–622.
Haggerty, R., Gorelick, S.M., 1995. Multiple-rate mass transfer for modeling diffusion and surface reactions in media with pore-scale heterogeneity. Water Resour. Res. 31 (10), 2383–2400.
Hansch, C., Leo, A., 1979. Substituent Constants for Correlation Analysis in Chemistry and Biology. Wiley, New York.
Harms, H., Zehnder, A.J.B., 1995. Bioavailability of sorbed 3-chlorodibenzofuran. Appl. Environ. Microbiol. 61 (1), 27–33.
Helfferich, F.G., Carr, P.W., 1993. Non-linear waves in chromatography: I. Waves, shocks and shapes. J. Chromatogr. 629, 97–122.
Holmén, B.A., Gschwend, P.M., 1997. Estimating sorption rates of hydrophobic organic compounds in iron oxide- and aluminosilicate clay-coated aquifer sands. Environ. Sci. Technol. 31 (1), 105–113.
Hu, Q., Brusseau, M.L., 1996. Transport of rate-limited sorbing solutes in an aggregated porous medium: A multiprocess non-ideality approach. J. Cont. Hydrol. 24, 53–73.
Jury, W.A., Flühler, H., 1992. Transport of chemicals through soil: mechanisms, models, and field applications. Adv. Agron. 47, 141–201.
Jury, W.A., Gardner, W.R., Gardner, W.H., 1991. Soil Physics. Wiley, New York.
Klausen, J., Tröber, S.P., Haderlein, S.B., Schwarzenbach, R.P., 1995. Reduction of substituted nitrobenzenes by Fe(II) in aqueous mineral suspensions. Environ. Sci. Technol. 29 (9), 2396–2404.
Klausen, J., Haderlein, S.B., Schwarzenbach, R.P., 1997. Oxidation of substituted anilines by aqueous MnO_2: effect of co-solutes on initial- and quasi steady state kinetics. Environ. Sci. Technol. 31 (9), 2642–2649.
Leo, A., Hansch, C., Elkins, D., 1971. Partition coefficients and their uses. Chem. Rev. 71, 702–709.

Maciejewski, S., 1993. Numerical and experimental study of solute transport in unsaturated soils. J. Cont. Hydrol. 14, 193–206.

Martell, A.E., Smith, R.M., 1982. Critical Stability Constants. Plenum Press, New York.

Martins, J.M., Mermoud, A., 1998. Sorption and degradation of four nitroraomatic herbicides in mono and multi-solute saturated/unsaturated soil batch systems. J. Cont. Hydrol. 33, 187–210.

McBride, J.F., Brockman, F.J., Szecsody, J.E., Streile, G.P., 1992. Kinetics of quinoline biodegradation, sorption and desorption in a clay-coated model soil containing a quinoline-degrading bacterium. J. Cont. Hydrol. 9, 133–154.

Miller, M.E., Alexander, M., 1991. Kinetics of bacterial degradation of benzylamine in a montmorillonite suspension. Environ. Sci. Technol. 25 (2), 240–245.

Nielsen, D.R., Biggar, J.W., 1961. Miscible displacement in soils: I. Experimental information. Soil Sci. Soc. Am. Proc. 25 (1), 1–5.

Ogram, A.V., Jessup, R.E., Ou, L.T., Rao, P.S.C., 1985. Effects of sorption on biological degradation rates of (2,4-dichlorophenoxy)acetic acid in soils. Appl. Environ. Microbiol. 49 (3), 582–587.

Parker, J.C., van Genuchten, M.T., 1984. Determining transport parameters from laboratory and field tracer experiments. Blacksburg, VA.

Reichert, P., 1994a. AQUASIM—A tool for simulation and data analysis of aquatic systems. Wat. Sci. Technol. 30 (2), 21–30.

Reichert, P., 1994b. Concepts underlying a Computer Program for the Identification and Simulation of Aquatic Systems. Swiss Federal Institute for Environmental Science and Technology (EAWAG), Dübendorf, Switzerland.

Russo, D., Dagan, G., 1991. On solute transport in a heterogeneous porous formation under saturated and unsaturated water flows. Water Resour. Res. 27 (3), 285–292.

Sahimi, M., Heiba, A.A., Davis, H.T., Scriven, L.E., 1986. Dispersion in flow through porous media: II. Two-phase flow. Chem. Eng. Sci. 41 (8), 2123–2135.

Schwarzenbach, R.P., Gschwend, P.M., Imboden, D.M., 1993. Environmental Organic Chemistry. Wiley, New York, pp. 194–200.

Serjeant, E.P., Dempsey, B., 1979. Ionisation Constants of Organic Acids in Aqueous Solution. Pergamon Press, Oxford.

Simon, W., Reichert, P., 1997. An extension of AQUASIM to saturated soil columns. Ground Water, submitted.

Stone, A.T., Torrents, A., Smolen, J., Vasudevan, D., Hadley, J., 1993. Adsorption of organic compounds possessing ligand donor groups at the oxide/water interface. Environ. Sci. Technol. 27 (5), 895–909.

Sugita, F., Gillham, R.W., 1995. Pore scale variation in retardation factor as a cause of nonideal reactive breakthrough curves: 1. Conceptual model and its evaluation. Water Resour. Res. 31 (1), 103–112.

Toride, N., Leij, F.J., van Genuchten, M.T., 1995. The CXTFIT Code for Estimating Transport Parameters from Laboratory or Field Tracer Experiments, Version 2.0. US Department of Agriculture, Riverside, CA, USA.

Torrents, A., Stone, A.T., 1991. Hydrolysis of phenyl picolinate at the mineral/water interface. Environ. Sci. Technol. 25, 143–149.

Unger, K.K.E., 1989. Handbuch der HPLC. Git Verlag, Darmstadt.

Weissmahr, K.W., Haderlein, S.B., Schwarzenbach, R.P., 1997. Complex formation of soil minerals with nitroaromatic explosives and other π-acceptors. Soil Sci. Soc. Am. J., in press.

Young, D.F., Ball, W.P., 1994. A priori simulation of tetrachloroethene transport through aquifer material using an intraparticle diffusion model. Environ. Prog. 13 (1), 9–20.

Zachara, J.M., Ainsworth, C.C., Smith, S.C., 1990. The sorption of *N*-heterocyclic compounds on reference and subsurface smectite clay isolates. J. Cont. Hydrol. 6, 281–305.

Zurmühl, T., Durner, W., Herrmann, R., 1991. Transport of phthalate-esters in undisturbed and unsaturated soil columns. J. Cont. Hydrol. 8, 111–133.